Title

Honours Literature Review

Thomas D. Schanzer
Supervisor: Prof. Steven Sherwood

School of Physics
Climate Change Research Centre and ARC Centre of Excellence for Climate Extremes
University of New South Wales, Sydney, Australia

Abstract

Text

Contents

1 Introduction

1.1 Traditional parametrisation schemes

2 Theory of parametrisation

3 Data-driven parametrisation schemes

4 Parametrisation development using toy models

5 Dynamical system case study: Rayleigh-Bénard convection

5.1 Problem statement

Rayleigh-Bénard convection is the motion of a fluid confined between two horizontal isothermal plates, the temperature of the bottom plate being higher than that of the top plate. The governing equations for the flow follow from the Navier-Stokes equations of mass, energy and momentum conservation. The reader is referred to Chandrasekhar (1961) for a detailed derivation; I summarise the assumptions and approximations involved below.

The density, ρ, of the fluid is related to its temperature T by the linear equation of state

$$\rho = \rho_0[1 - \alpha(T - T_0)],$$

where α is the (constant) volume coefficient of thermal expansion and ρ_0 and T_0 are the base-state density and temperature such that $\rho = \rho_0$ when $T = T_0$. The key assumption is that density variations are small ($\alpha(T - T_0) \ll 1$), which allows the governing equations to be simplified under the *Boussinesq approximation*. The Boussinesq approximation involves first writing the pressure, p, of the fluid as

$$p = p_0 - \rho_0 g z + p',$$

where p_0 is an arbitrary constant, g is the acceleration due to gravity and z is the vertical coordinate. p' is the (time-varying) deviation from a hydrostatically balanced background profile $p_0 - \rho_0 g z$ in which the upward pressure gradient force per unit volume $\rho_0 g$ cancels the downward weight force per unit volume $-\rho_0 g$. Since $\alpha(T - T_0) \ll 1$, density variations are neglected everywhere except in their contribution to the weight force, leading to a net buoyant (background pressure gradient plus weight) force per unit mass

$$\frac{\rho_0 - \rho}{\rho_0} g = \alpha(T - T_0) g.$$

With these assumptions in mind, I adopt the governing equations as they are derived by Chandrasekhar (1961):

$$\frac{\partial \boldsymbol{u}}{\partial t} + \boldsymbol{u} \cdot \boldsymbol{\nabla} \boldsymbol{u} = -\frac{1}{\rho_0} \boldsymbol{\nabla} p' + \alpha(T - T_0) g \hat{\boldsymbol{z}} + \nu \nabla^2 \boldsymbol{u} \quad \text{(momentum conservation)}, \tag{5.1}$$

$$\frac{\partial T}{\partial t} + \boldsymbol{u} \cdot \boldsymbol{\nabla} T = \kappa \nabla^2 T \quad \text{(energy conservation), and} \tag{5.2}$$

$$\boldsymbol{\nabla} \cdot \boldsymbol{u} = 0 \quad \text{(incompressibility)}. \tag{5.3}$$

$\boldsymbol{u}$ is the fluid velocity, t is time, $\hat{\boldsymbol{z}}$ is the upward unit vector, ν is the (constant) kinematic viscosity and κ is the thermal diffusivity (also constant). Notice that the aforementioned buoyancy term $\alpha(T - T_0)g$ appears on the right-hand side of (5.1).

The parametrisation test-bed developed in this work solves the governing equations in a two-dimensional domain $(x, z) \in [0, d] \times [0, L]$, subject to no-slip, isothermal boundary conditions on the top and bottom plates,

$$\boldsymbol{u} = \boldsymbol{0}, \quad T = T_0 + \frac{\delta T}{2} \qquad \text{at } z = 0 \text{ and} \tag{5.4}$$

$$\boldsymbol{u} = \boldsymbol{0}, \quad T = T_0 - \frac{\delta T}{2} \qquad \text{at } z = d, \tag{5.5}$$

and periodic boundary conditions in the horizontal,

$$\boldsymbol{u}(x = 0) = \boldsymbol{u}(x = L) \quad \text{and} \quad T(x = 0) = T(x = L). \tag{5.6}$$

δT is the constant temperature difference between the plates.

5.2 Nondimensionalisation and scale analysis

It is helpful to nondimensionalise the governing equations (5.1)–(5.6); this is not only useful for numerical work but also gives insight into the different flow regimes that are possible. A range of nondimensionalisations are used in fluid dynamics literature; I adopt a common one (see, e.g., Grötzbach (1983), Ouertatani et al. (2008), and Stevens, Verzicco, and Lohse (2010)) which is suitable for the turbulent convective regime.

For low-viscosity, turbulent flow, a suitable time scale is the *free-fall time* t_0, which is the time for a fluid element with constant temperature $T = T_0 - \delta T$ to fall from the top plate to the bottom plate under the influence of buoyancy ($-g\alpha\delta T$) alone. It is simple to show that

$$t_0 \sim \left(\frac{d}{g\alpha\delta T}\right)^{1/2},$$

ignoring a factor of $\sqrt{2}$. The obvious length and temperature scales are the plate separation d and temperature difference δT, respectively.

Making the substitutions $p'/\rho_0 \to \pi$ and $T - T_0 \to \theta$ in (5.1)–(5.6) and expressing all variables in units of t_0, d and δT leads to the dimensionless equations

$$\frac{\partial \boldsymbol{u}}{\partial t} + \boldsymbol{u}\cdot\boldsymbol{\nabla}\boldsymbol{u} = -\boldsymbol{\nabla}\pi + \left(\frac{\mathrm{Pr}}{\mathrm{Ra}}\right)^{1/2}\nabla^2\boldsymbol{u} + \theta\hat{\boldsymbol{z}}, \tag{5.7}$$

$$\frac{\partial \theta}{\partial t} + \boldsymbol{u}\cdot\boldsymbol{\nabla}\theta = (\mathrm{Ra}\,\mathrm{Pr})^{-1/2}\nabla^2\theta, \quad \text{and} \tag{5.8}$$

$$\boldsymbol{\nabla}\cdot\boldsymbol{u} = 0, \tag{5.9}$$

with boundary conditions

$$\boldsymbol{u} = \boldsymbol{0}, \quad \theta = +\frac{1}{2} \qquad \text{at } z = 0, \tag{5.10}$$

$$\boldsymbol{u} = \boldsymbol{0}, \quad \theta = -\frac{1}{2} \qquad \text{at } z = 1, \tag{5.11}$$

$$\boldsymbol{u}(x=0) = \boldsymbol{u}(x=\Gamma) \quad \text{and} \quad \theta(x=0) = \theta(x=\Gamma). \tag{5.12}$$

There are three dimensionless parameters: the aspect ratio of the domain

$$\Gamma \equiv \frac{L}{d},$$

the *Prandtl number*

$$\mathrm{Pr} \equiv \frac{\nu}{\kappa}$$

which measures the relative importance of viscosity (momentum diffusivity) and thermal diffusivity, and the *Rayleigh number*

$$\mathrm{Ra} \equiv \frac{g\alpha d^3\delta T}{\kappa\nu}.$$

The Rayleigh number can be interpreted as the ratio of the time scale for thermal transport by convection to the time scale for thermal transport by conduction. It determines the importance of diffusion for the evolution of $\boldsymbol{u}$ and θ; inspection of (5.7) and (5.8) indicates that low Ra implies strong diffusion and high Ra weak diffusion. Detailed theoretical analysis of the governing equations (see, e.g., Chandrasekhar (1961) and the seminal work by Lord Rayleigh (1916)) reveals that there exists a critical Rayleigh number (dependent on boundary conditions but of order 10^3), below which the equations have a stable equilibrium with the fluid at rest and a linear conductive temperature profile. Above the critical value, the equilibrium is unstable and small perturbations lead to the formation of a regular series of steady, rotating convection cells. If the Rayleigh number is increased much further (Le Quéré (1991) cites $\mathrm{Ra} \approx 2 \times 10^8$), the solution becomes unsteady and increasingly turbulent. This work is concerned with the turbulent regime, since Rayleigh numbers for atmospheric deep moist convection can be as large as 10^{22} (Chillà and Schumacher 2012).

5.3 Thermal properties

The rate of heat transport across the fluid layer has physical significance for natural realisations of thermally driven convection. It is widely analysed in terms of the dimensionless *Nusselt number*, whose accurate determination is a common theme in the Rayleigh-Bénard convection literature; I therefore introduce this quantity before proceeding. The Nusselt number measures the rate of (vertical) heat transport across a horizontal plane at height z, normalised by the purely conductive rate that would exist if the fluid were at rest (Verzicco and Camussi 1999). Following Chillà and Schumacher (2012), I use the definition (before nondimensionalisation)

$$\mathrm{Nu}(z,t) \equiv \frac{\langle wT\rangle_{A,t} - \kappa\partial\langle T\rangle_{A,t}/\partial z}{\kappa\delta T/d} \tag{5.13}$$

where $\langle\cdot\rangle_{A,t}$ denotes averaging over time and the horizontal plane at height z, and $w = \boldsymbol{u}\cdot\hat{\boldsymbol{z}}$ is the vertical velocity. The rate of heat transport in the numerator has two terms: advection $\langle wT\rangle_{A,t}$ and conduction $-\kappa\partial\langle T\rangle_{A,t}/\partial z$. The denominator $\kappa\delta T/d$ is the rate of heat transport for a linear conductive temperature profile with the fluid at rest. Scheel, Emran, and Schumacher (2013) give the corresponding nondimensionalised form,

$$\mathrm{Nu}(z,t) \equiv (\mathrm{Ra}\,\mathrm{Pr})^{1/2}\langle w\theta\rangle_{A,t} - \frac{\partial\langle\theta\rangle_{A,t}}{\partial z}. \tag{5.14}$$

Another important quantity is the thickness δ_T of the *thermal boundary layer* at each plate where large temperature gradients exist. Chillà and Schumacher (2012) define δ_T as follows: if, on average, the fluid temperature changes with height from $+\delta T/2$ at the lower plate to 0 (the mean value in the well-mixed interior) over a distance δ_T, then

$$\left.\frac{\partial\langle T\rangle_{A,t}}{\partial z}\right|_{z=0} \approx -\frac{\delta T}{2\delta_T}.$$

But if one considers the definition of the Nusselt number (5.13) at $z = 0$, the advection term $\langle wT\rangle_{A,t}$ vanishes due to the $\boldsymbol{u} = \boldsymbol{0}$ boundary condition and

$$\mathrm{Nu}(z=0) = -\frac{d}{\delta T}\left.\frac{\partial\langle T\rangle_{A,t}}{\partial z}\right|_{z=0}.$$

Thus,

$$\delta_T = \frac{d}{2\,\mathrm{Nu}(z=0)}. \tag{5.15}$$

5.4 Resolution dependence of numerical solutions

In constructing a parametrisation test-bed, I will firstly seek reasonably accurate, high-resolution "truth" solutions of (5.7)–(5.12). I will then deliberately reduce the resolution, aiming to produce solutions that are sufficiently "different" that they might reasonably be "improved" by a parametrisation scheme. In this section, I review relevant literature with the aim of establishing how, exactly, under-resolved simulations of Rayleigh-Bénard convection might "differ" from well-resolved ones, and thus what one would hope to "improve". Specifically, I will address the following questions:

- What resolution is necessary for a converged solution?
- Which quantities are most sensitive to insufficient resolution?

5.4.1 Theoretical resolution requirements for accurate simulations

Grötzbach (1983) is recognised as the first to formulate resolution requirements for accurate simulations of Rayleigh-Bénard convection (Chillà and Schumacher 2012; Scheel, Emran, and Schumacher 2013). He

identified separate constraints on the mean (i.e., averaged in each spatial direction) grid spacing and the vertical spacing near the plates; we first discuss the former. Grötzbach reasoned that a numerical model that neglects subgrid-scale effects must have a geometric mean grid spacing $h = (\Delta x \Delta y \Delta z)^{1/3}$ such that

$$h \leq \pi\eta = \pi \left(\frac{\nu^3}{\langle \epsilon \rangle} \right)^{1/4} \tag{5.16}$$

where $\eta \equiv (\nu^3/\epsilon)^{1/4}$ is the *Kolmogorov length*, the universal smallest relevant length scale for general turbulent flow, and $\langle \epsilon \rangle$ is the spatial and temporal average of the kinetic energy dissipation rate defined by

$$\epsilon(\boldsymbol{x}, t) \equiv \frac{\nu}{2} \sum_{ij} \left(\frac{\partial u_i}{\partial x_j} + \frac{\partial u_j}{\partial x_i} \right)^2 \tag{5.17}$$

(Chillà and Schumacher 2012). The condition (5.16) can be understood using the Nyquist-Shannon theorem, which states that a sampling frequency $f \geq k/\pi$ is needed to unambiguously reconstruct a signal with wavenumber k; substituting $f = 1/h$, $k = 1/\eta$ leads to the claimed relation.

Grötzbach recognised that the above reasoning was only valid for the mean grid spacing; large gradients in temperature and velocity near the top and bottom plates require finer resolution in those regions. The notion of nearness can be formalised using the thermal boundary layer thickness (5.15), and one asks how many grid points are necessary in this layer. Grötzbach did not give a theoretical argument to derive this number but claimed that 3 points are sufficient for turbulent flows. Shishkina et al. (2010) presented a theoretical argument based on the (experimentally and numerically justified) assumption of laminar *Prandtl-Blasius* flow conditions in the boundary layer and were able to calculate the minimum number of grid points (e.g., 9 for $\mathrm{Ra} = 2 \times 10^9$ and $\mathrm{Pr} = 0.7$). The results agreed with criteria derived in previous numerical experiments. Importantly, the results of Shishkina et al. allow *a priori* determination of vertical resolution requirements, potentially bypassing the time-consuming and expensive process of iteratively running simulations, checking their convergence and updating the resolution.

5.4.2 Resolution-dependence tests and consequences of under-resolution

Performing numerical experiments for a 3D fluid layer, Grötzbach found that RMS velocity and Nusselt number were the most sensitive quantities to insufficient mean grid spacing, but even they increased "only slightly" above the values obtained from well-resolved simulations. He concluded that condition (5.16) was overly restrictive and recommended (for $\mathrm{Pr} > 0.59$) the simplified, approximate version

$$h \lesssim 5.23\,\mathrm{Pr}^{-1/4}\mathrm{Ra}^{-0.3205}.$$

Later work also supports the finding that the Nusselt number is sensitive to under-resolution. Even studying only steady-state convective solutions at moderate Rayleigh number, Le Quéré (1991) found that the maximum and minimum Nusselt numbers were most sensitive to changes in resolution and had the largest uncertainty among existing benchmark solutions. Other studies have used the convergence of the Nusselt number as an indicator that the spatial resolution is sufficient to produce an accurate solution (Ouertatani et al. 2008).

Stevens, Verzicco, and Lohse (2010) performed 3D simulations in a finite cylindrical cavity with the aim of reconciling the apparent disagreement between the Nusselt numbers in previous numerical studies and experimental observations. They found that agreement with experiment could be achieved, but only by using a much higher resolution than the previous studies. They offered the physical explanation that horizontally under-resolved simulations produce insufficient thermal diffusion, leading to systematic overestimation of the buoyancy of convective plumes near the side-walls of the cylinder; this results in Nusselt numbers that exceed experimentally observed values. This led them to conclude that the two criteria of Grötzbach (1983)—for mean grid spacing and for the vertical spacing near the upper and lower plates—are not independent; the definition $h = (\Delta x \Delta y \Delta z)^{1/3}$ in (5.16) allows the horizontal spacing to remain relatively coarse near the plates, provided the vertical spacing is small. Since fine horizontal

resolution is also necessary to accurately capture the dynamics of the thin plumes, they proposed that (5.16) be applied with $h = \max(\Delta x, \Delta y, \Delta z)$ instead.

Some more recent work, however, casts doubt on the notion that the Nusselt number is sensitive to under-resolution and that its convergence is a good indicator that the flow is well-resolved. In assessing the performance of several published computational fluid dynamics codes on the Rayleigh-Bénard problem in a cylindrical cavity, Kooij et al. (2018) identified one higher-order code that reproduced the theoretically predicted scaling of Nu as a function of Ra even when the flow was deliberately under-resolved. On the other hand, the presence of numerical artefacts in the instantaneous temperature field near the bottom plate was a clear indicator of insufficient resolution. Figure 1, a reproduction of part of their Figure 5, shows these artefacts.

Scheel, Emran, and Schumacher (2013) performed similar high-resolution simulations for a cylindrical cavity and also found that the Nusselt number, among other global transport properties, were "fairly insensitive to insufficient resolution, as long as the mean Kolmogorov length [was] resolved" (i.e., (5.16) was satisfied). However, they found that the horizontally averaged or local kinetic energy dissipation rate (5.17) and the corresponding thermal dissipation rate

$$\epsilon_T(\boldsymbol{x}, t) \equiv \kappa \sum_i \left(\frac{\partial T}{\partial x_i} \right)^2 \tag{5.18}$$

were much more sensitive, with their convergence requiring even stricter conditions than (5.16).

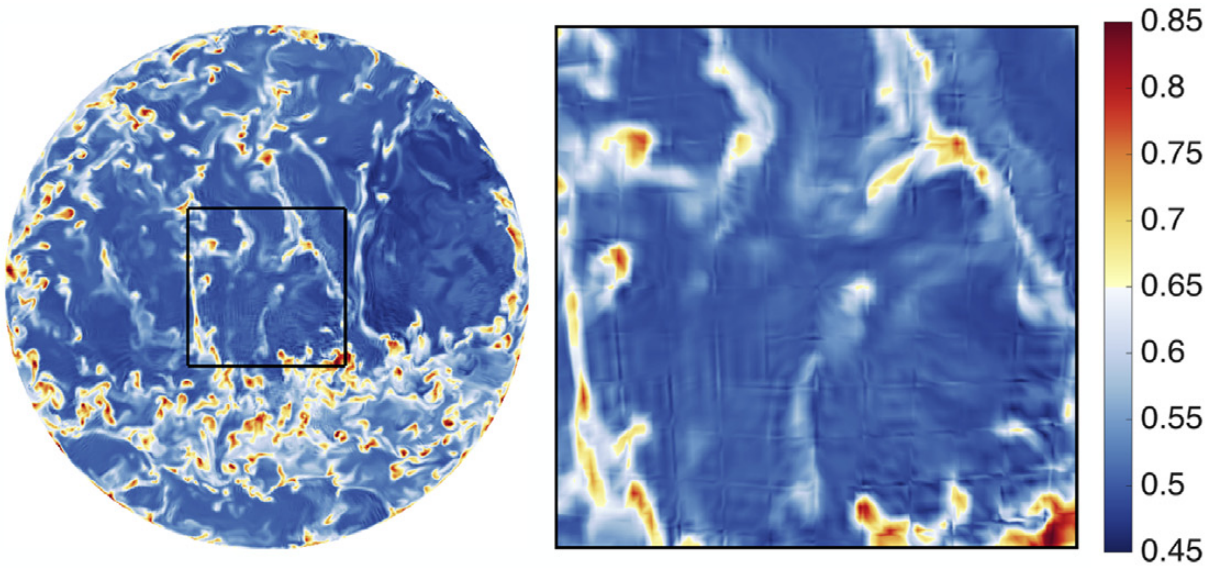

Figure 1: Reproduction of part of Figure 5 by Kooij et al. (2018), showing an instantaneous horizontal temperature profile simulated by the Nek5000 code for Rayleigh-Bénard convection at $\mathrm{Ra} = 10^{10}$. The profile is taken near the bottom plate of a cylindrical cavity and shows a grid-like pattern of numerical artefacts. The right panel is an enlargement of the region inside the black square in the left panel.

6 Conclusion

References

Chandrasekhar, S. (1961). *Hydrodynamic and hydromagnetic stability*. Oxford: Clarendon Press. ISBN: 9780486319209.

Chillà, F. and J. Schumacher (2012). "New perspectives in turbulent Rayleigh-Bénard convection". *Eur. Phys. J. E* **35**(7). DOI: 10.1140/epje/i2012-12058-1.

Grötzbach, G. (1983). "Spatial resolution requirements for direct numerical simulation of the Rayleigh-Bénard convection". *J. Comput. Phys.* **49**(2). DOI: 10.1016/0021-9991(83)90125-0.

Kooij, G. L., M. A. Botchev, E. M. A. Frederix, B. J. Geurts, S. Horn, D. Lohse, E. P. van der Poel, O. Shishkina, R. J. A. M. Stevens, and R. Verzicco (2018). "Comparison of computational codes for direct numerical simulations of turbulent Rayleigh-Bénard convection". *Comput. Fluids* **166**. DOI: 10.1016/j.compfluid.2018.01.010.

Le Quéré, P. (1991). "Accurate solutions to the square thermally driven cavity at high Rayleigh number". *Comput. Fluids* **20**(1). DOI: 10.1016/0045-7930(91)90025-D.

Lord Rayleigh (1916). "On convection currents in a horizontal layer of fluid, when the higher temperature is on the under side". *Philos. Mag.* **32**(192). DOI: 10.1080/14786441608635602.

Ouertatani, N., N. Ben Cheikh, B. Ben Beya, and T. Lili (2008). "Numerical simulation of two-dimensional Rayleigh-Bénard convection in an enclosure". *C.R. Mec.* **336**(5). DOI: 10.1016/j.crme.2008.02.004.

Scheel, J. D., M. S. Emran, and J. Schumacher (2013). "Resolving the fine-scale structure in turbulent Rayleigh-Bénard convection". *New J. Phys.* **15**(11). DOI: 10.1088/1367-2630/15/11/113063.

Shishkina, O., R. J. A. M. Stevens, S. Grossmann, and D. Lohse (2010). "Boundary layer structure in turbulent thermal convection and its consequences for the required numerical resolution". *New J. Phys.* **12**(7). DOI: 10.1088/1367-2630/12/7/075022.

Stevens, R. J. A. M., R. Verzicco, and D. Lohse (2010). "Radial boundary layer structure and Nusselt number in Rayleigh-Bénard convection". *J. Fluid Mech.* **643**. DOI: 10.1017/S0022112009992461.

Verzicco, R. and R. Camussi (1999). "Prandtl number effects in convective turbulence". *J. Fluid Mech.* **383**. DOI: 10.1017/S0022112098003619.